

Supporting Information

Strongly-coupled PbS QD solids by Doctor Blading for IR Photodetection

Alberto Maulu^a, Pedro J. Rodríguez-Cantó^{b,*}, Juan Navarro-Arenas^a, Rafael Abarques^b, Juan F. Sánchez-Royo^a, Raúl García-Calzada^a, and Juan P. Martínez Pastor^{a,*}

^aInstituto de Ciencia de los Materiales, Universidad de Valencia, P.O. Box 22085, 46071 Valencia, Spain

*E-mail: Juan.Mtnez.Pastor@uv.es

^bINTENANOMAT S.L., C/Catedrático José Beltrán 2, 46980 Paterna, Spain

*E-mail: pedro.j.rodriguez@uv.es

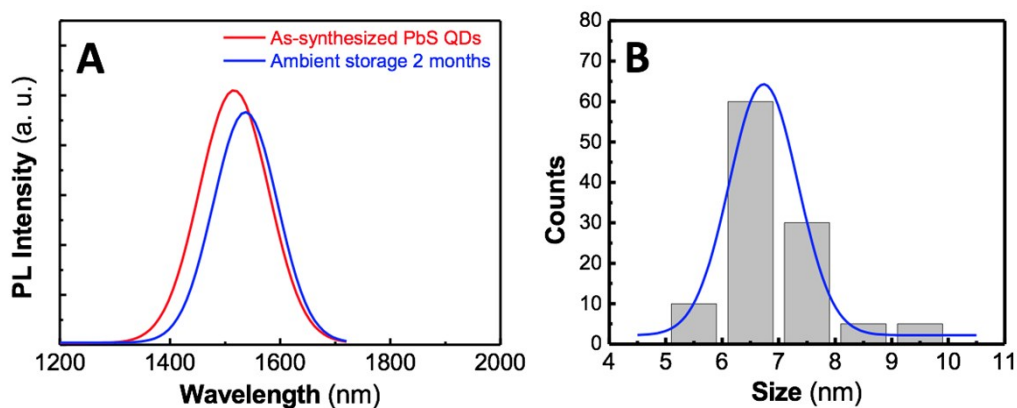


Figure S1. a) Photoluminescence spectra of a freshly prepared PbS QD solution before and after two months. b) Size histogram of the colloidal PbS QDs. The mean size equals 6.5 nm, with a size dispersion of 8.5 %.

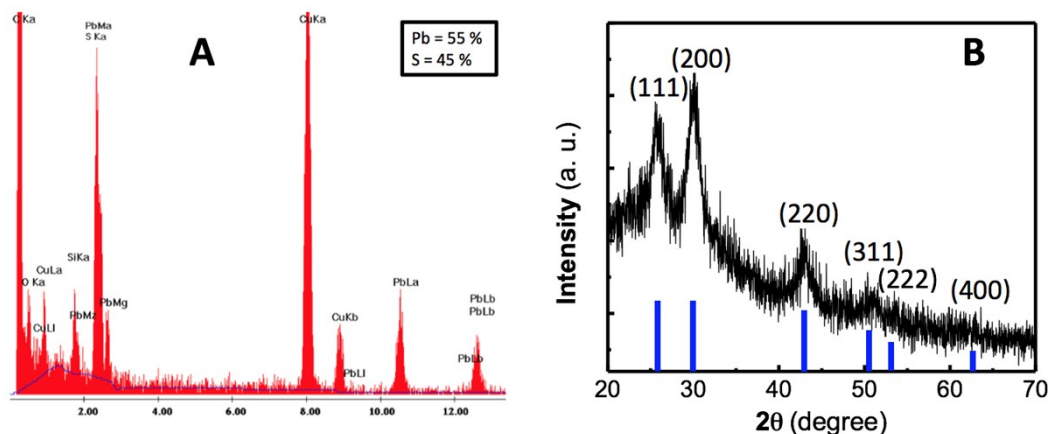


Figure S2: a) EDX analysis and b) X-Ray Diffraction pattern of PbS QDs.

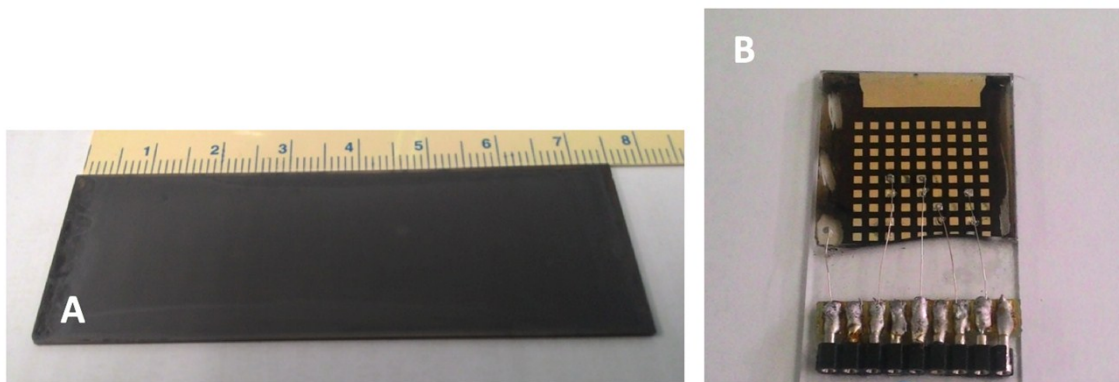


Figure S3: a) Photographs of a QD solid film produced by doctor blading on a 7.5 x 2.5 cm² substrate and b) an array of photodiodes fabricated on a 3 x 2.5 cm² sample from the middle of the sample.

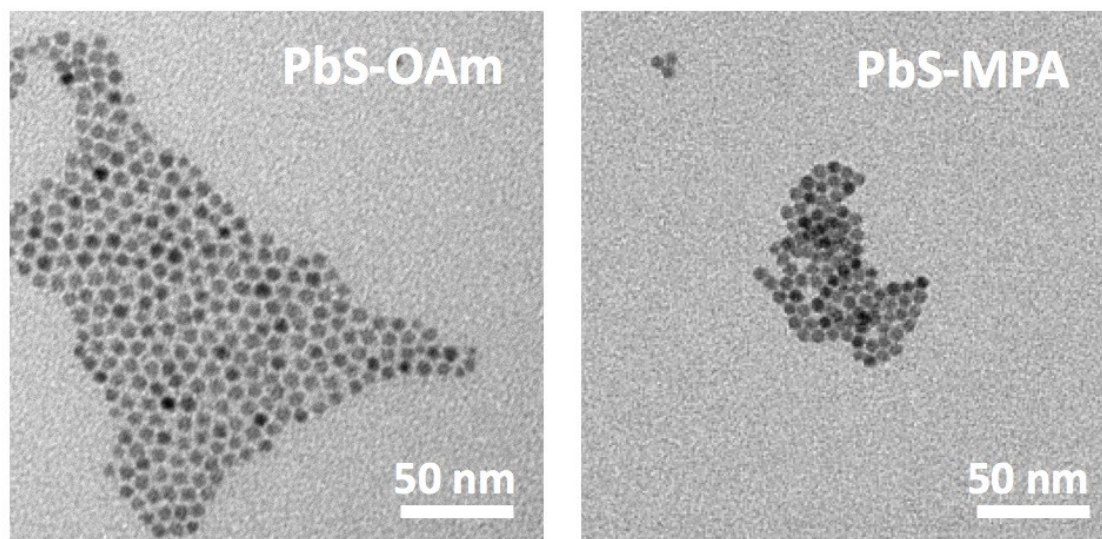


Figure S4: TEM images of PbS QDs before (left) and after the ligand exchange process (right). Image analysis of the images reveals an interparticle separation of OAm-capped PbS QDs (6.7 nm in diameter) of 2.3 nm, which is significantly reduced to 0.7 nm after the ligand exchange.

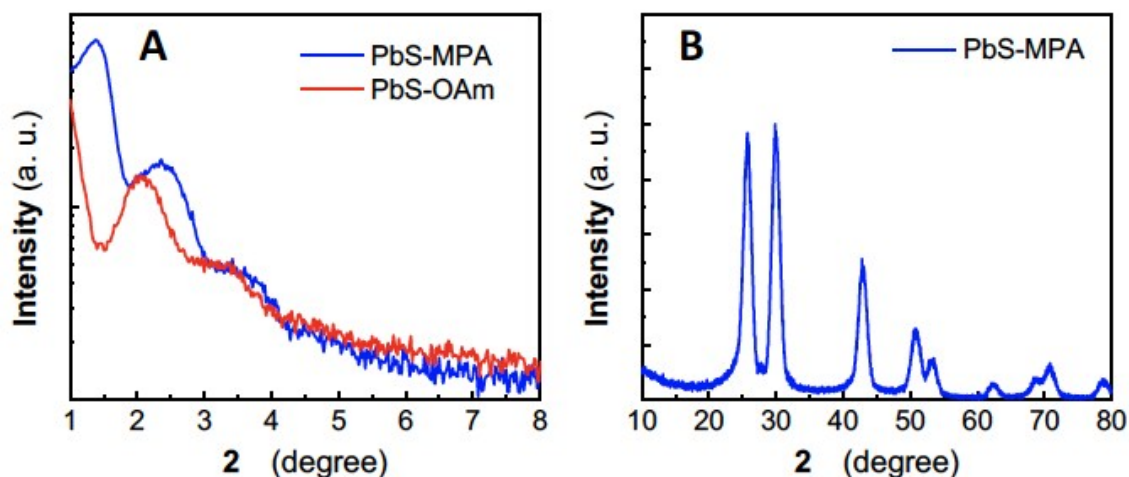


Figure S5. a) Low-angle X-Ray diffraction pattern of OAm-capped (red line) MPA-capped (blue line) PbS QD solid films prepared by doctor blading (*) and b) GIXD obtained for the MPA-capped PbS QDs in the same doctor blading film as in a) (this pattern is quite similar to that measured for OAm-capped PbS QDs shown in Fig. 1e).

(*) Low-angle X-ray diffraction pattern provides diffraction patterns associated to the superlattice formed by self-organization of the QDs during deposition onto the substrate. In the sample with MPA-capped PbS QDs three main diffracting planes are observed at $2\theta \approx 1.38, 2.37$ and 3.43° . The corresponding superlattice planes would be (110), (211) and (222), respectively, of a body-centered cubic (BCC) Bravais lattice. The lattice constant of the non-primitive cubic unit cell turns to be $a = 9.05$ nm, from which we obtain a diameter of 7.8 nm for solid spheres (D) forming the lattice, which is consistent with the sum of the QD diameter plus the MPA ligand length, approximately. In the case of the OAm-capped PbS QDs, given that we only observe two diffraction angles (greater than 1°) at $2\theta \approx 2.05$ and 3.19° , we make the assumption that QD-ligand units self-organize into a BCC structure and hence these angles would correspond to diffracting planes (211) and (222), respectively. From this assignation we would deduce a lattice constant $a \approx 10.5$ nm and hence $D = 9.1$ nm, which is consistent with the higher length of OAm ligands as compared to MPA ones.

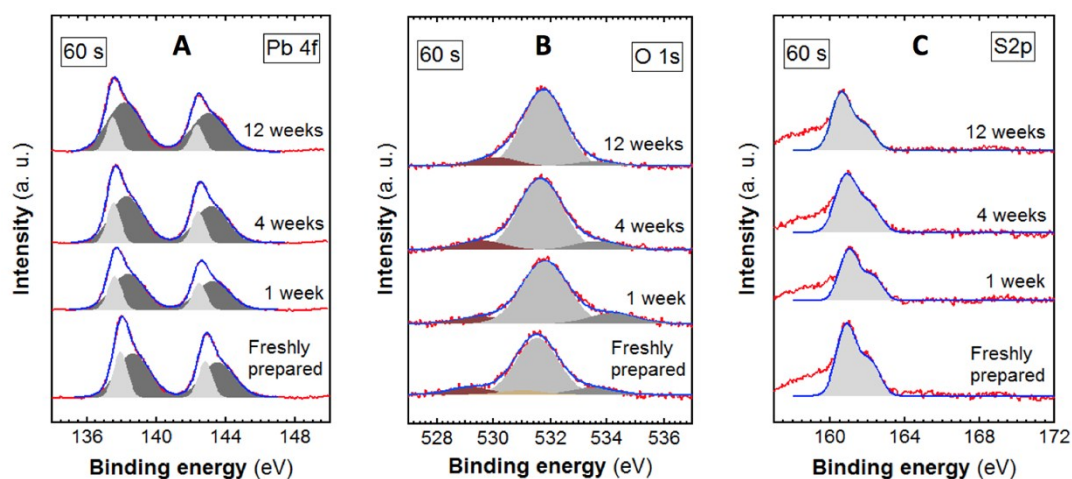


Figure S6: XPS measurements of the PbS QD solids exposed to air for different times: a) Pb 4f, b) O 1s and c) S 2p spectra.

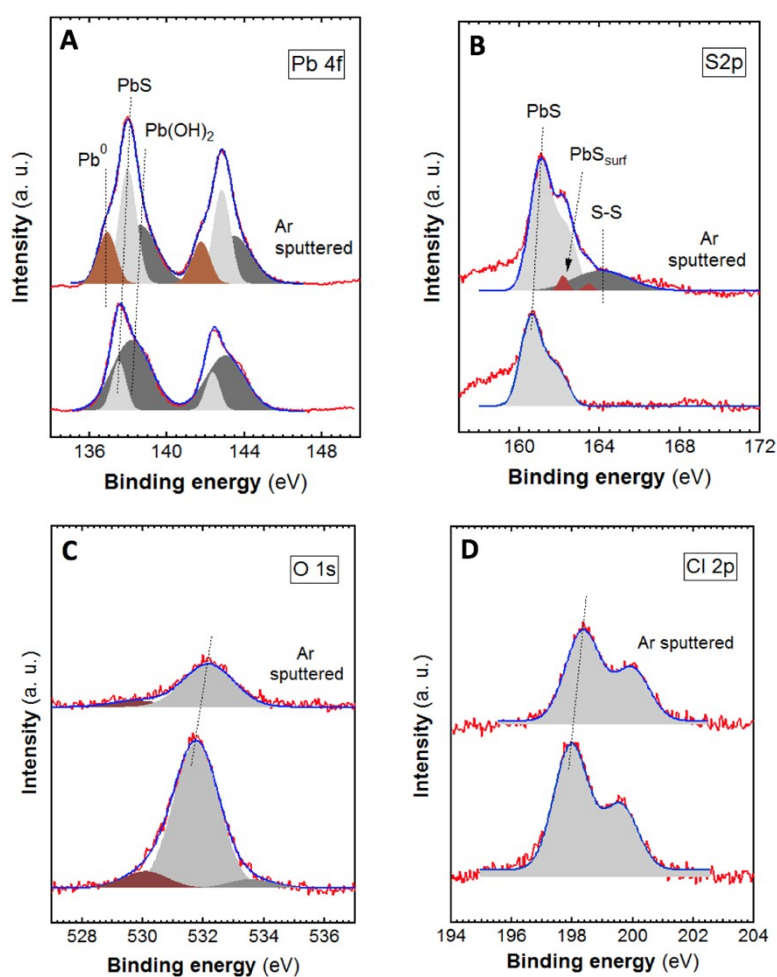


Figure S7: XPS measurements of the PbS QD solids before and after Ar⁺ sputtering in ultrahigh-vacuum: a) Pb 4f, b) S 2p, c) O 1s and d) Cl 2p spectra. The samples were prepared under 60 s of ligand exchange treatment and kept in air for 3 months.

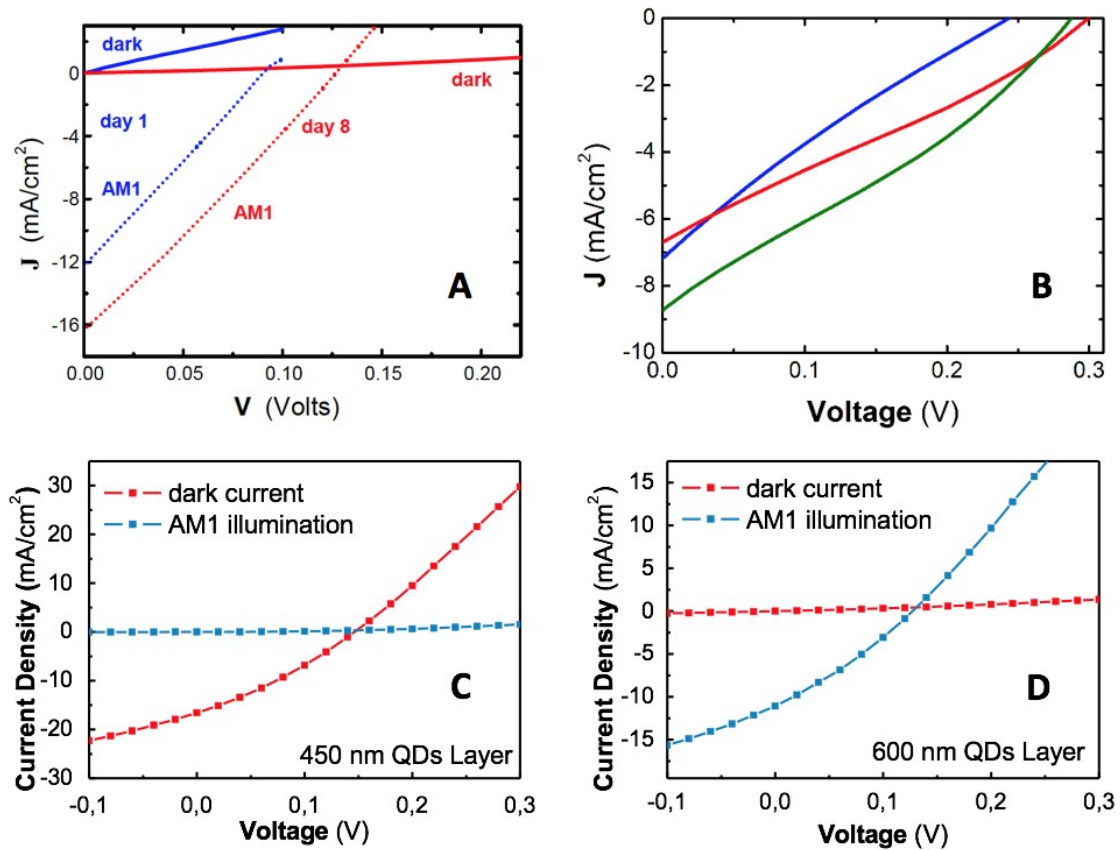


Figure S8: I-V curves under dark and AM1.5 illumination conditions (as indicated in the plot) in several samples without encapsulation: a) as-prepared and after 8 days under low-vacuum conditions, b) several diodes of the sample (depicted in Figure S3b) where the highest V_{OC} where obtained, c)-d) two diodes of the sample where the highest photocurrents where obtained.

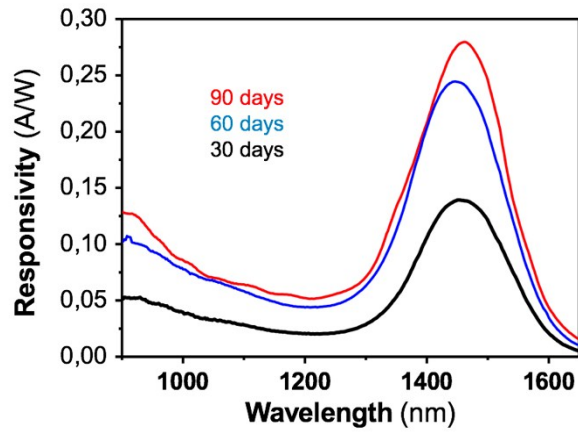


Figure S9: Responsivity spectra of the studied encapsulated photodetector in air for 10 (black), 50 (green) and 90 (red) days.

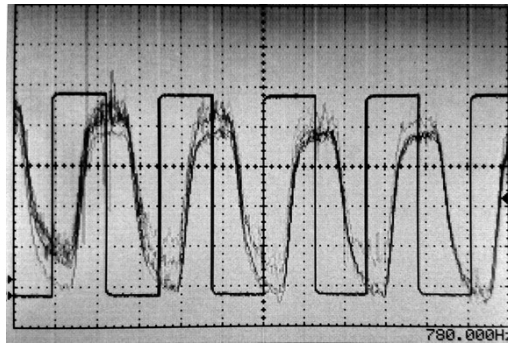


Figure S10: Photocurrent transient response measured at 0 V under chopped light at 780 Hz.

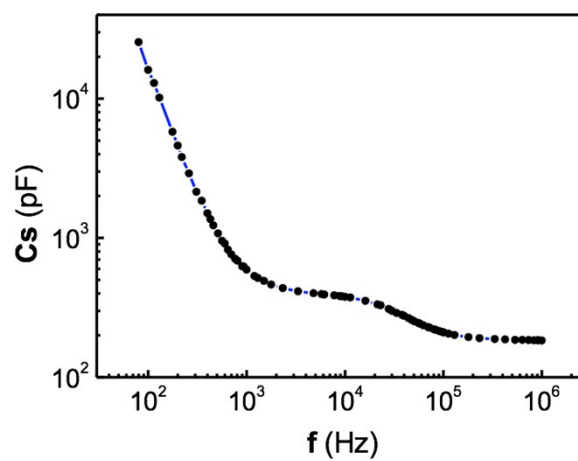


Figure S11: Capacitance as a function of the probe signal frequency measured at 0 V using a LCR meter.

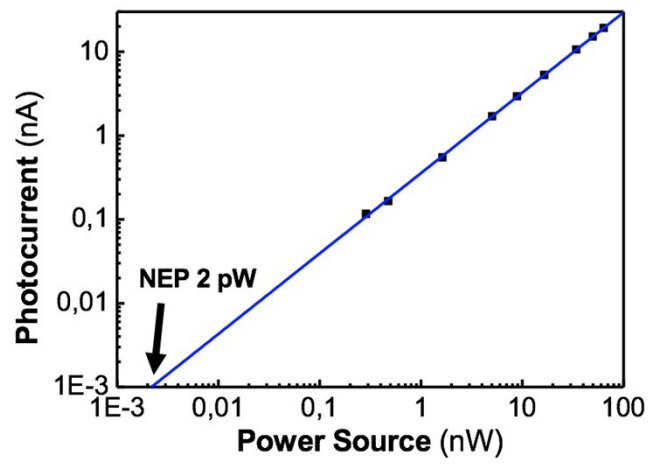


Figure S12: Photocurrent measured as a function of the incident optical power at 1550 nm.